The Heart as an Acoustic Dipole: Spatiotemporal Mapping of the Cardiac Acoustic Activity on the Chest

Noemi Giordano[1], Samuel E. Schmidt[1], Marco Knaflitz[2], Johannes J. Struijk[1]

[1]Department of Health Science and Technology, Aalborg University, Aalborg, Denmark
[2]Department of Electronics and Telecommunications, Politecnico di Torino, Torino, Italy

Abstract

Digital auscultation is a promising tool to monitor cardiac hemodynamics, but traditional single-point recordings are highly sensitive to sensor placement. Knowledge of the morphological difference of the signals across the chest is still very sparse. We present a spatiotemporal analysis of the evolution of the heart sounds over the chest utilizing a wearable 58-channel microphone array covering the left hemithorax. Mapping the acoustic field of the first (S1) and second (S2) heart sounds reveals the heart is not an isotropic acoustic source. Instead, topographic mapping shows distinct spatial phase inversions indicative of a directional mechanical dipole. A combination of Principal Component Analysis and anisotropic 2D Gaussian modelling was used to quantify the directionality of the trajectory of the instantaneous intensity centroid. The principal direction was found to lie between 40° and 90° within the hexaxial reference system, compatible with the heart's anatomical longitudinal axis. These findings highlight the importance of sensor placement in traditional PCG and lay the foundations for a comprehensive mapping of the cardiac acoustic activity.

1. Introduction

Even though more modern techniques have partially replaced its role in diagnosis, digital auscultation has strong potential for point-of-care screening and home monitoring of many cardiovascular conditions. Moreover, digital phonocardiography (PCG) enables the extraction of features beyond the possibilities of the human ear, e.g., Cardiac Time Intervals, providing new acoustic-based insights into cardiac hemodynamics.

Traditionally, auscultation is performed over specific auscultation areas, resulting from decades of clinical expertise. These areas are optimized to best auscultate the cardiac murmurs, but are not necessarily optimal for all purposes. In fact, the detection of PCG fiducial marks depends on the signal morphology which is not necessarily the same all over the chest. The problem is widely understudied: most works dealing with PCG do not state the stethoscope position and the standardization over the sample population. Among publicly available datasets, only CirCor [1] provides stethoscope locations. In this context, understanding how the morphology of the cardiac acoustic waves evolves across the thorax remains a significant open challenge. While multi-channel PCG offers a valuable tool to capture this spatiotemporal evolution, few studies have deployed dense arrays of microphones. Furthermore, existing acoustic mapping efforts, such as those by Guo et al. [2] and Sapsanis et al. [3], primarily map the absolute acoustic energy. By disregarding signal polarity, these approaches lose critical phase information, treating the heart as an isotropic acoustic source rather than a complex system.

To address this gap, this work analyses the spatiotemporal evolution of the two main heart sounds with a high spatial and temporal resolution. Utilizing a custom prototype equipped with 58 microphones, we track the trajectory of the acoustic intensity centroid over time. By combining Principal Component Analysis (PCA) with anisotropic 2D Gaussian modeling, we quantify the directionality of this spatial trajectory. Our analysis shows that the cardiac acoustic field manifests as a highly directional dipole, creating phase inversion across the chest, whose principal axis aligns with the expected direction of the longitudinal axis of the heart.

2. Materials and Methods

2.1. Multi-channel recording of heart sounds

High-spatial-resolution acoustic recordings were performed using a prototype developed at Politecnico di Torino. The prototype was built upon the hardware architecture described in [4]. It embeds an expanded array of 58 electret condenser microphones on a flexible printed circuit board (PCB) to be located over the patient's left hemithorax. The microphones (6-mm diameter, 16-mm inter-microphone distance) are arranged in a high-resolution, homogeneous grid covering the traditional

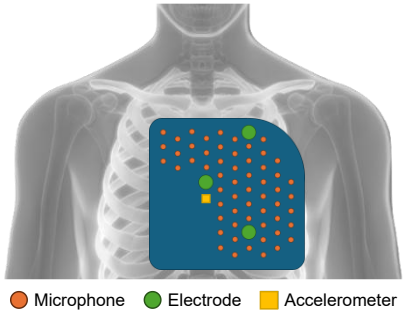

Figure 1. Position of the sensors over the chest.

auscultation areas. The device also records a synchronized electrocardiogram and tri-axial acceleration, with all signals sampled at 1 kHz. Figure 1 shows the position of the sensors and the placement on the chest.

For this study, one-minute recordings were obtained from: a) eight healthy volunteers; b) one healthy subject recorded daily for 8 consecutive days.

2.2. Topographic mapping of the instantaneous sound intensity

For each recording, all 58 channels were band-pass filtered between 30 Hz and 100 Hz, the bandwidth were the contributions of the first (S1) and second (S2) heart sounds are most prevalent. S1 and S2 were segmented using a duration-dependent hidden Markov model [5], and arranged in two matrices. The following was applied independently for S1 and S2.

The physical geometry of each array was mapped to a Cartesian coordinate system, creating a grid where the sensor's physical position was translated into a (x,y) point. To evaluate the continuous spatial distribution of the acoustic activity over the chest, discrete sensor amplitudes were interpolated onto a uniform, high-resolution 2D mesh grid using biharmonic spline interpolation. To prevent extrapolation outside the physical boundaries of the array, a spatial mask corresponding to the convex hull of the outermost sensor coordinates was applied.

A heatmap was created for each time instant with the heart sound. In other words, for each instant the heatmap represents the instantaneous amplitude of the sound in the corresponding chest location. Amplitudes were normalized with min-max scaling, using the global minimum and maximum to respect the differences across channels. Figure 2 shows an example for an S2 sound.

2.2. Estimation of the intensity centroid

To pinpoint the spatial epicenter of the acoustic field at any given instant, the intensity centroid (IC) was calculated for each temporal frame. For frame t, the IC coordinates were computed as the spatial center of mass of the squared relative amplitudes:

$$x_{IC}(t) = \frac{\sum x \cdot s^2(t,x,y)}{\sum s^2(t,x,y)}, y_{IC}(t) = \frac{\sum y \cdot s^2(t,x,y)}{\sum s^2(t,x,y)}$$

where $s(t,x,y)$ is the amplitude of the sound at time instant t at coordinates (x,y). Squaring is employed to

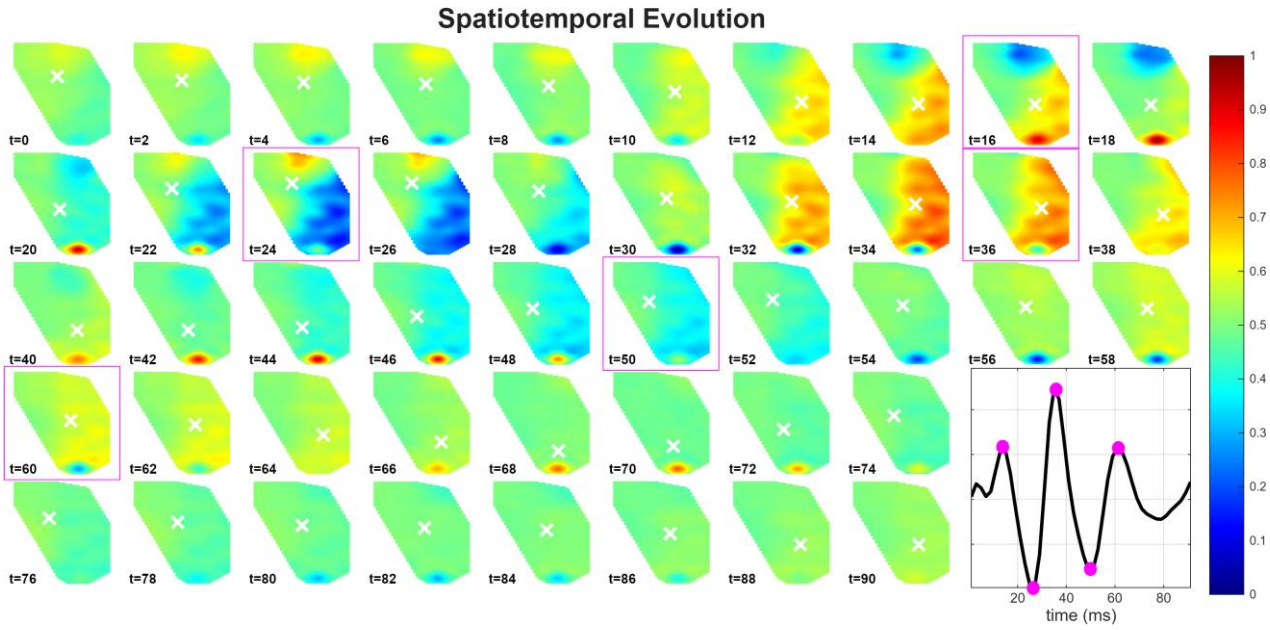

Figure 1. The heatmaps show the spatial distribution of the intensity of an S2 at 45 time instants between t = 0 (corresponding to the estimated start of S2) and t = 90 ms. The average S2 is plotted for reference, with maxima and minima highlighted in magenta. The corresponding heatmaps are squared in the same color.

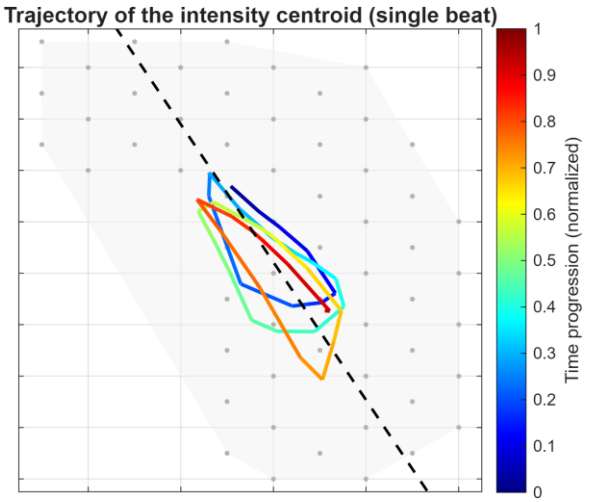

Figure 3. Trajectory of the IC on a sample S2. The gray area represents the surface of the physical array.

highlight the sound with respect to spatial background noise. Figure 2 shows the position of the IC estimated for each frame as a white cross on the heatmap.

Tracking the IC across successive temporal frames yields a spatial trajectory of the acoustic epicenter for the specific sound. Figure 3 shows the trajectory of the estimated IC over time. It can be observed that the trajectory shows a clear directionality.

2.3. Estimation of the principal direction

To robustly characterize the distribution and directionality of the cardiac acoustic field, IC trajectories were aggregated across multiple heartbeats. To quantify the spatial distribution, Principal Component Analysis (PCA) was applied in conjunction with an anisotropic 2D Gaussian model. First, the overall average and the 2-by-2 covariance matrix were computed. Then, to extract the primary axes of movement, PCA was performed via eigenvalue decomposition of the covariance matrix. The first principal component (i.e., the eigenvector associated with the maximum eigenvalue $\sigma_{max}{}^2$) represents the dominant spatial axis of IC movement, from which the global principal direction was derived and represented by its angle. The second principal component represents the orthogonal, minor axis of spatial dispersion with variance $\sigma_{min}{}^2$.

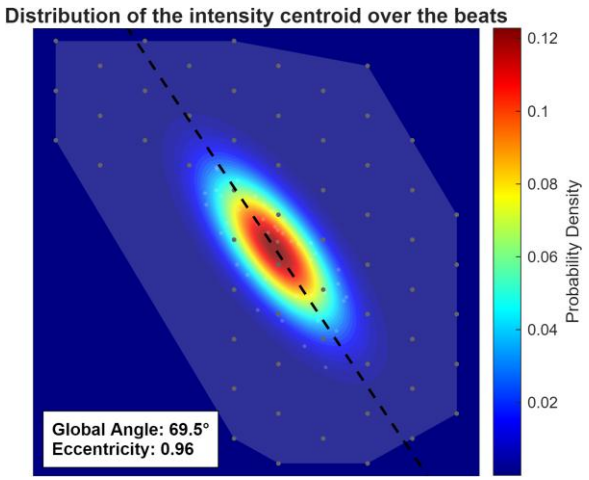

Figure 4. Distribution of the intensity centroid over all S2s from one subject. The probability density corresponds to its anisotropic 2D Gaussian modelling.

To quantify the linearity and directionality of the acoustic trajectories, the eccentricity of the distribution was calculated as:

$$eccentricity = \sqrt{1 - \left(\frac{\sigma_{min}}{\sigma_{max}}\right)^2}$$

An eccentricity close to 1 indicates a highly linear, tightly constrained directional trajectory, whereas a value close to 0 indicates a diffuse, circular distribution with no strong directionality.

Finally, the Mahalanobis distance was calculated for all IC points relative to the Gaussian model and a probability density contour map over the sensor array was generated and visualized. Figure 4 shows an example of the IC contour map of the S2 sound previously reported.

3. Results

Figure 5 presents the estimated angles of the principal direction of respectively S1 and S2 over the sample population. It can be observed that all angles for both sounds lie between 40° and 90° within the hexaxial reference system (where 0° represents the patient's left and 90° represents the inferior direction), compatible with the direction of the cardiac axis. The eccentricity values were always higher than 0.8, showing that the directionality is very strong. It can also be observed that there is a good agreement between the principal direction extracted from S1 and the one extracted from S2 from the same subject (same color in Figure 5). The mean angular difference between S1 and S2 was -0.26°, showing no systematic bias, with a median absolute difference of 2.2°. No evidence of a systematic difference was observed with a paired Student's t-test ($p = 0.64$), while the small angular differences support good agreement between the two measurements. These results suggest that the observed directionality is consistent across S1 and S2 and may therefore be related to subject-specific anatomy.

In the end, Table I summarizes the results of the analysis when applied to the same subjects on daily recordings. Also in this case, high eccentricity values confirm high directionality. The principal direction over different days is very stable. Small differences are most likely due to a slightly different orientation of the recording device over different days.

4. Discussion and conclusions

The proposed analysis aims to move beyond traditional single-point digital auscultation to explore the spatio-temporal evolution of acoustic intensity over the chest during S1 and S2. We show both qualitatively and quantitatively that the acoustic field does not manifest as a simple isotropic acoustic radiator, but rather as a highly directional dipole. The first evidence of this dipolar behavior is visible in the topographic mapping of the acoustic intensity: the spatial maps consistently reveal distinct phase inversions across the chest wall. This dipolar behavior was further quantified by tracking the dynamic trajectory of the IC across multiple heartbeats. The fitted anisotropic 2D Gaussian models exhibited high spatial eccentricity, confirming that the acoustic epicenter does not move randomly or uniformly but it is highly constrained to oscillate along a dominant direction. Crucially, the principal axis of the observed acoustic dipole aligns with the expected direction of the anatomical longitudinal axis of the heart. Since S1 and S2 are primarily generated by the closure of the heart valves, the physical vibrations and pressure waves are expected to propagate perpendicular to the valves. Consequently, the acoustic energy radiates bidirectionally along the heart's longitudinal axis, matching the principal direction mapped in our spatiotemporal analysis.

The spatial propagation of the sounds over the chest is highly underexplored, but carries tremendous implications for the clinical practice: if the recordings on different points are not simply scaled versions of the same signal, but present phase shift or inversion, the selection of the recording point becomes a critical source of variability.

The presented findings are limited by a small sample population: future work will expand the analysis to a larger dataset and validate the alignment between the estimated principal direction and the subject's cardiac axis via imaging or other modalities.

Subj	Angle (deg)	ecc.
S1	65,3	0,96
S2	62,6	0,96
S3	50,5	0,82
S4	68,2	0,94
S5	70,4	0,96
S6	59,4	0,92
S7	64,0	0,96
S8	81,3	0,96

Subj	Angle (deg)	ecc.
S1	65,5	0,96
S2	62,6	0,96
S3	41,6	0,81
S4	65,4	0,88
S5	67,8	0,95
S6	61,2	0,83
S7	68,7	0,93
S8	88,3	0,93

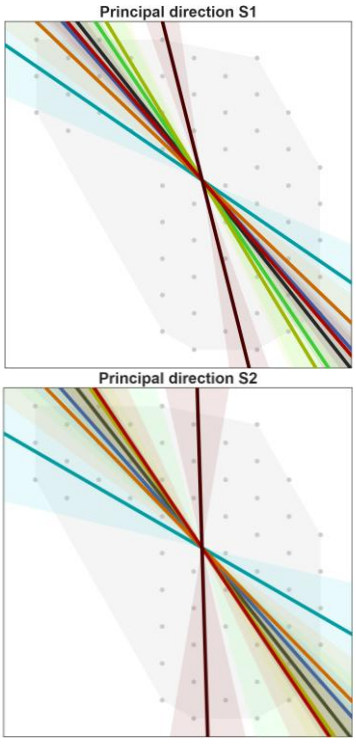

Figure 5. Angle of the principal direction of respectively S1 and S2 over the sample population.

Table 1. Angle of the principal direction resulting from daily recordings on the same subject.

Day	S1			S2		
	avg (deg)	std (deg)	ecc.	avg (deg)	std (deg)	ecc.
1	82.2	3.4	0.97	77.1	4.8	0.95
2	79.3	1.9	0.98	79.7	3.1	0.96
3	80.4	5.9	0.92	69.8	4.6	0.95
4	75.8	3.1	0.95	71.2	2.5	0.96
5	81.4	2.3	0.98	77.6	2.2	0.97
6	83.5	3.7	0.95	79.4	2.6	0.94
7	78.1	7.2	0.95	71.9	6.6	0.94
8	84.7	2.3	0.99	76.9	2.1	0.98

Acknowledgments

The work was funded by the European Union via MSCA Postdoctoral Fellowship (GA 101207722).

References

[1] J. Oliveira *et al.*, "The CirCor DigiScope Phonocardiogram Dataset," *PhysioNet*, Jan. 2022.

[2] B. Guo, H. Tang, S. Xia, M. Wang, Y. Hu, and Z. Zhao, "Development of a multi-channel wearable heart sound visualization system," *J. Pers. Med.*, vol. 12, no. 12, p. 2011, 2022.

[3] C. Sapsanis *et al.*, "StethoVest: A simultaneous multichannel wearable system for cardiac acoustic mapping," in *2018 IEEE Biomedical Circuits and Systems Conference (BioCAS)*, 2018, pp. 1–4.

[4] N. Giordano, *et al.*, "A wearable multi-sensor array enables the recording of heart sounds in homecare," *Sensors*, vol. 23, no. 13, p. 6241, 2023.

[5] S. E. Schmidt, *et al.*, "Segmentation of heart sound recordings by a duration-dependent hidden Markov model," *Physiol. Meas.*, vol. 31, no. 4, pp. 513–529, 2010.

Address for correspondence:

Noemi Giordano
Department of Health Science and Technology, Aalborg University, Selma Lagerløfs Vej 249, 9260 Gistrup, Denmark.
nogi@hst.aau.dk